Scintigraphic Imaging of Infectious Foci with an ^{111}In-LTB4 Antagonist Is Based on In Vivo Labeling of Granulocytes

Julliëtte E.M. van Eerd, MSc[1]; Wim J.G. Oyen, MD[1]; Thomas D. Harris, PhD[2]; Huub J.J.M. Rennen, PhD[1]; D. Scott Edwards, PhD[2]; Frans H.M. Corstens, MD[1]; and Otto C. Boerman, PhD[1]

[1]*Department of Nuclear Medicine, University Medical Centre Nijmegen, Nijmegen, The Netherlands; and* [2]*Discovery Research, Bristol-Myers Squibb Medical Imaging, North Billerica, Massachusetts*

Radiolabeled leukotriene B4 (LTB4) antagonist DPC11870 is able to reveal infectious and inflammatory foci in distinct animal models. Because previous studies showed that accumulation of ^{111}In-DPC11870 in the abscess continued although the tracer had cleared from the circulation, we decided to investigate the pharmacodynamics of ^{111}In-DPC11870 and determine the mechanism of accumulation of the radiolabeled LTB4 antagonist in the abscess. **Methods:** ^{111}In-DPC11870 was intravenously injected in healthy New Zealand White rabbits and rabbits with intramuscular *Escherichia coli* infection. Pharmacodynamics were studied by serial imaging and by ex vivo counting of dissected tissues. The mechanism of visualization of the abscess was investigated in rabbits with intramuscular infection that was induced 16 h after intravenous administration of ^{111}In-DPC11870. In addition, heterologous leukocytes and bone marrow cells of a donor rabbit were labeled with ^{111}In-DPC11870 in vitro and the biodistribution of these in vitro radiolabeled cells was compared with that of ^{111}In-DPC11870 in rabbits with an infection. **Results:** The LTB4 antagonist ^{111}In-DPC11870 revealed the intramuscular abscess in rabbits only a few hours after injection. Quantitative analysis of the images confirmed accumulation of ^{111}In-DPC11870 in the abscess although the compound had cleared almost completely from the circulation. Radioactivity concentration in the bone marrow decreased more rapidly in infected animals than in healthy animals. Therefore, we hypothesized that ^{111}In-DPC11870 associates with receptor-positive (bone marrow) cells and accumulated in the abscess because of subsequent migration from the bone marrow to the abscess. Accumulation of radioactivity in the abscess induced 16 h after ^{111}In-DPC11870 injection was similar to that in animals intravenously injected with the tracer 24 h after induction of the abscess (0.37 ± 0.16 percentage injected dose [%ID]/g). Moreover, differences in radioactivity concentration in the bone marrow of healthy and infected animals (0.67 ± 0.29 %ID/g and 0.15 ± 0.03 %ID/g at 24 h, respectively, after injection) supported our hypothesis. Additional studies with peripheral blood leukocytes and bone marrow cells that were labeled ex vivo with ^{111}In-DPC11870 showed the ability of these cells to migrate to the abscess (0.40 %ID/g and 0.52 %ID/g for ^{111}In-DPC11870 bone marrow cells and ^{111}In-DPC11870 peripheral blood leukocytes, respectively, 24 h after injection). **Conclusion:** The ^{111}In-labeled LTB4 antagonist DPC11870 accumulates in infectious and inflammatory foci because of binding to LTB4 receptors expressed on activated hematopoietic cells that subsequently migrate to the site of infection, which leads to visualization of the infectious lesions.

Key Words: LTB4 antagonist; infection imaging; scintigraphy

J Nucl Med 2005; 46:786–793

Detection of infectious and inflammatory foci by scintigraphic imaging is important because it allows accurate therapeutic decisions and rapid initiation of treatment. Radiolabeled leukocytes are currently considered the gold standard to detect infectious and inflammatory lesions in patients (*1*). This radiopharmaceutical enables rapid visualization of the lesion, but preparation is time consuming and associated with a potential risk for infection (*2*). At the moment, there is interest in the development of new radiopharmaceuticals to detect infectious and inflammatory foci with the same accuracy as radiolabeled leukocytes but without these disadvantages. Chemotactic and chemokinetic peptides are promising agents for this application (*3,4*). These compounds have the potential to accumulate at the site of infection and are cleared rapidly from nontarget tissues and from the circulation. Various studies, however, indicate that the use of these agonistic compounds is often limited because of biologic activity, whereas antagonists often exhibit low receptor affinity (*5*). We have developed a leukotriene B4 (LTB4) antagonist, DPC11870, that can be labeled with ^{111}In and that reveals infectious and inflammatory lesions rapidly after injection (*4,6*).

LTB4 is a potent chemotactic factor for granulocytes that, on binding to its specific cell surface receptors, stimulates leukocyte functions such as chemotaxis, vascular adhesion, transendothelial migration, and release of lysosomal enzymes (*7,8*). Because LTB4 is an important mediator and

Received Aug. 20, 2004; revision accepted Oct. 21, 2004.

For correspondence or reprints contact: Julliëtte E.M. van Eerd, MSc, Department of Nuclear Medicine, University Medical Center Nijmegen, P.O. Box 9101, 6500 HB Nijmegen, The Netherlands.

E-mail: J.vaneerd@nucmed.umcn.nl

LTB4 receptors are expressed by polymorphonuclear granulocytes, we investigated the imaging potential of a bivalent LTB4 antagonist. We have shown that this radiolabeled antagonist could reveal infectious and inflammatory foci in various rabbit models (*6,9,10*). Results also demonstrated that ^{111}In-DPC11870 cleared rapidly from the circulation. Furthermore, we demonstrated that visualization of the lesions was possible within a few hours after injection of the radiolabel. In vivo receptor-blocking experiments showed that accumulation and retention at the site of infection was receptor mediated.

The aim of this study was to elucidate the mechanism of ^{111}In-DPC11870 accumulation in the abscess. Initial experiments were performed to determine the pharmacokinetics of ^{111}In-DPC11870, and additional biodistribution experiments were performed to determine the mechanism of accumulation in the abscess.

MATERIALS AND METHODS

Radiolabeling of DPC11870

DPC11870 was synthesized and characterized as described previously (*6,10*). The LTB4 antagonist DPC11870 was labeled with ^{111}In with a specific activity of 3.7 MBq/μg DPC11870 (12 MBq/nmol). Quality control of the compound was performed with instant thin-layer chromatography and high-performance liquid chromatography as described previously (*6*).

Infection Model

Nineteen female New Zealand White rabbits weighing 2.3–2.8 kg were kept in cages (1 rabbit per cage) and fed standard laboratory chow and water ad libitum. An *Escherichia coli* infection was induced in the left thigh muscle of 11 animals by intramuscular injection of 1×10^{11} colony-forming units of *E. coli*. During this procedure, the rabbits were anesthetized by subcutaneous injection of 0.7 mL of a mixture of 0.315 mg of fentanyl per milliliter and 10 mg of fluanisone per milliliter (Hypnorm; Janssen Pharmaceutica). All animal experiments were approved by the local animal welfare committee in accordance with the Dutch legislation and performed in accordance with their guidelines.

Whole-Body Imaging and Pharmacokinetics

Twenty-four hours after the induction of the infection, when swelling of the infected muscle was apparent, 5 rabbits (2 with intramuscular infection and 3 healthy) received an intravenous injection of 11 MBq of ^{111}In-DPC11870 (3 μg) in the lateral ear vein. For scintigraphic imaging, the rabbits were immobilized in a mold and placed prone on a dual-head Siemens Multi-SPECT II γ-camera equipped with a medium-energy parallel-hole collimator. The camera was connected to a Scintiview image processor and ICON computer system (Siemens). Scanning (11 cm/min over 70 cm) was performed immediately and at various time points up to 24 h after injection, and images were stored digitally in a 256 × 256 matrix. All images were adjusted to the same background and intensity level, to allow a fair comparison among the various experiments. The pharmacodynamics of ^{111}In-DPC11870 were studied by analyzing the images quantitatively. Regions of interest (ROIs) were drawn over the total body, heart, abscess, contralateral muscle (background), lungs, liver, spleen, kidneys, and lumbar spine (bone marrow). For each organ, except the bone marrow, the arithmetic mean value of the anterior and posterior regions was used. For bone marrow, only the posterior ROI was used. ROIs were used to calculate the ^{111}In-DPC11870 concentrations in the organs at the various time points. The percentage injected dose (%ID) in each organ was calculated using the total counts in the ROI of the organ and the whole-body counts. Because it was not possible to draw a region over the total amount of bone marrow, we calculated the %ID by using the amount of radioactivity measured after dissection. The correlation between the %ID found in the bone marrow and the average counts in the ROI was determined by linear regression analysis. Subsequently, the %ID in the bone marrow at all imaging time points was calculated by using this correlation data (slope and *y*-axis intercept).

After acquisition of the last image (24 h after injection) the animals were sacrificed with a lethal dose of sodium phenobarbital to determine the biodistribution of the agent. A blood sample was taken by cardiac puncture. Tissues were dissected and weighed. The activity in tissues was measured in a shielded well-type γ-counter along with the injection standards and was expressed as the %ID per gram (%ID/g) or %ID per organ (%ID).

Studies to Determine Mechanism of Accumulation in Abscess

To examine the mechanism of accumulation of the tracer in the abscess in more detail, we gave intravenous injections of 11 MBq of ^{111}In-DPC11870 (3 μg) to 10 healthy rabbits. Sixteen hours after the injection of the radiolabel, all animals were imaged and a blood sample was taken. After this procedure, in 5 of these animals an intramuscular *E. coli* infection was induced in the left thigh muscle as described above. Images of the healthy and infected animals were acquired from 1 h after abscess induction up to 24 h to determine accumulation of radioactivity at the site of the emerging infection, whereas the concentration of ^{111}In-DPC11870 in the circulation was very low. For scintigraphic imaging, the rabbits were immobilized in a mold and placed prone on a γ-camera (Orbiter; Siemens) using a medium-energy parallel-hole collimator. Images (300,000 counts per image) were acquired up to 24 h after induction of the abscess (i.e., 40 h after injection of the radiolabel) and stored digitally in a 256 × 256 matrix. All images were windowed identically (collection of 300,000 counts; same background and intensity level), allowing a fair comparison among the various experiments. After completion of the imaging experiment, the animals were sacrificed and biodistribution of the radiolabel was determined as already described.

^{111}In-DPC11870 Bound to White Blood Cells (WBCs) and Bone Marrow Cells (BMCs)

For the isolation and purification of the heterologous WBCs (*11*) and BMCs, a donor rabbit with an intramuscular *E. coli* infection was used. Twenty-four hours after induction of the abscess, 50 mL of heparinized blood were collected and granulocytes were isolated as described previously (*12*). The donor rabbit was sacrificed with an overdose of phenobarbital, and BMCs were isolated from both femurs. The BMCs were harvested and resuspended in 5 mL of phosphate-buffered saline containing 0.5% bovine serum albumin (w/v) (PBS/BSA). Cells were centrifuged for 10 min at 500*g*. The lipid layer and supernatant were removed. Peripheral WBCs and BMCs were washed twice with 50 mL of incubation buffer (1 mmol/L NaH_2PO_4, 5 mmol/L Na_2HPO_4, 140 mmol/L NaCl, 0.5 mmol/L $MgCl_2$, 0.15 mmol/L $CaCl_2$, 0.5% BSA, pH 7.4) and resuspended in 1 mL of incubation buffer. Both cell suspensions were incubated with 750 μL of ^{111}In-DPC11870

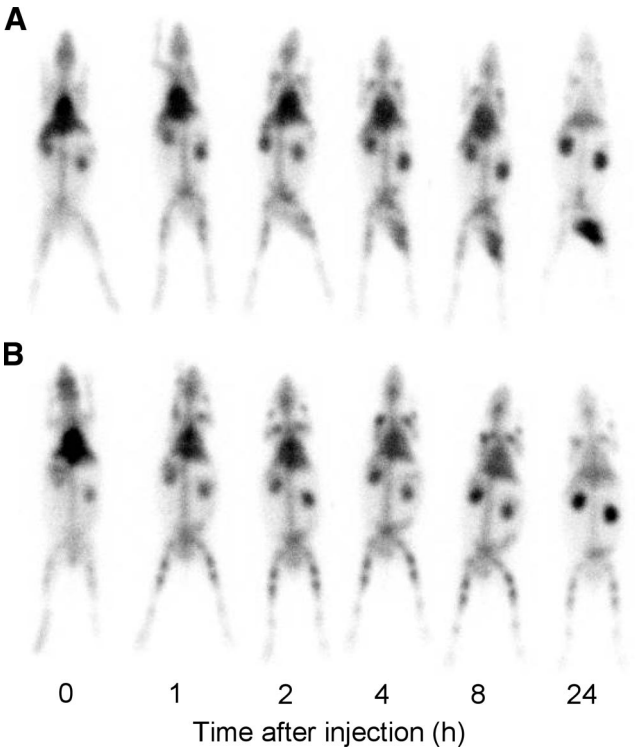

FIGURE 1. Whole-body images of rabbit with *E. coli* thigh muscle infection (A) and healthy rabbit (B) (anterior images are shown). Rabbits received 11 MBq of ^{111}In-DPC11870 (3 μg) intravenously. Images were acquired immediately and 1, 2, 4, 8 and 24 h after injection of ^{111}In-DPC11870.

(30 MBq) in incubation buffer for 15 min at room temperature. After the incubation, cells were washed twice with 10 mL of incubation buffer and resuspended in 2.5 mL of PBS/BSA. The amount of cell-bound radioactivity was determined.

Three rabbits with intramuscular *E. coli* infection (induced 24 h before) received an intravenous injection of either 4 MBq of ^{111}In-DPC11870 (1 μg), 4 MBq of ^{111}In-DPC11870–labeled WBCs, or 4 MBq of ^{111}In-DPC11870–labeled BMCs. The in vitro–radiolabeled WBCs and BMCs were intravenously injected to determine whether these ^{111}In-DPC11870–targeted cells would accumulate at the site of infection. Scintigraphic imaging and analysis of the images were performed as described above. The rabbits were sacrificed 24 h after injection of the radiolabel, and biodistribution was determined as already described.

Statistical Analysis

Regression analysis was performed on the data obtained from the biodistribution and on the ROI data obtained from the images. The correlation between these 2 parameters was calculated for each organ. Regression analysis was used to calculate the %ID present in the organs at the various time points.

All mean values are presented as mean ± SD. Statistical analysis was performed using the 2-sided Student *t* test. The level of significance was set at 0.05.

RESULTS

Radiolabeling of DPC11870

Reverse-phase high-performance liquid chromatography analysis and instant thin-layer chromatography quality control indicated that in all experiments the radiochemical purity of ^{111}In-DPC11870 exceeded 99%.

Whole-Body Imaging and Pharmacokinetics

The whole-body images acquired up to 24 h after injection of ^{111}In-DPC11870 demonstrated accumulation of the tracer in the abscess from a few hours after the injection (Fig. 1). The images also showed that the compound cleared rapidly from the circulation. The radiolabeled LTB4 antagonist showed some physiologic uptake in bone marrow and spleen and retention of radioactivity in the kidneys. Remarkably, the images displayed ongoing accumulation of radiolabeled compound in the abscess even when the majority of the compound had cleared from the circulation (>4 h after injection). Comparing the images acquired from healthy rabbits with those from rabbits with intramuscular infection, we saw no major differences in the distribution of ^{111}In-DPC11870. The biodistribution data are summarized in Figure 2. They confirmed the relatively high uptake of the radiolabeled antagonist in the abscess, bone marrow, and spleen. Distinct differences in radioactivity concentration were found in bone marrow and spleen of healthy and infected animals (0.67 ± 0.29 %ID/g vs. 0.15 ± 0.03 %ID/g in bone marrow [$P = 0.011$] and 1.14 ± 0.17 %ID/g vs. 0.27 ± 0.05 %ID/g in spleen [$P = 0.007$], for healthy and infected animals, respectively). For each organ the regression analysis showed a good correlation between the 2 datasets (ROI-based uptake vs. uptake in dissected tissues). Correlation coefficients were high for most tissues (r = 0.97, 0.93, 0.70, 0.80, 0.94, 0.71, and 0.99 for kidney, bone marrow, lung, liver, spleen, heart, and muscle and abscess, respectively). The pharmacodynamics of ^{111}In-DPC11870 for each organ is depicted in Figure 3. The curves of a few organs, however, displayed some remarkable features. Almost immediately after injection, uptake of ^{111}In-DPC11870 was observed in lungs, liver, kidneys, spleen, and bone

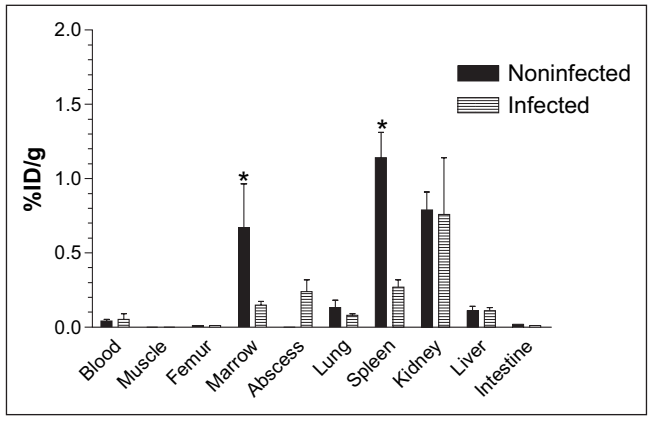

FIGURE 2. Biodistribution data obtained 24 h after injection of ^{111}In-DPC11870 in healthy rabbits (noninfected) and rabbits with intramuscular abscess (infected). Each bar represents mean value ± SD. Unpaired *t* test was used to analyze values for differences in uptake of radiolabel between healthy and infected animals. *$P < 0.05$.

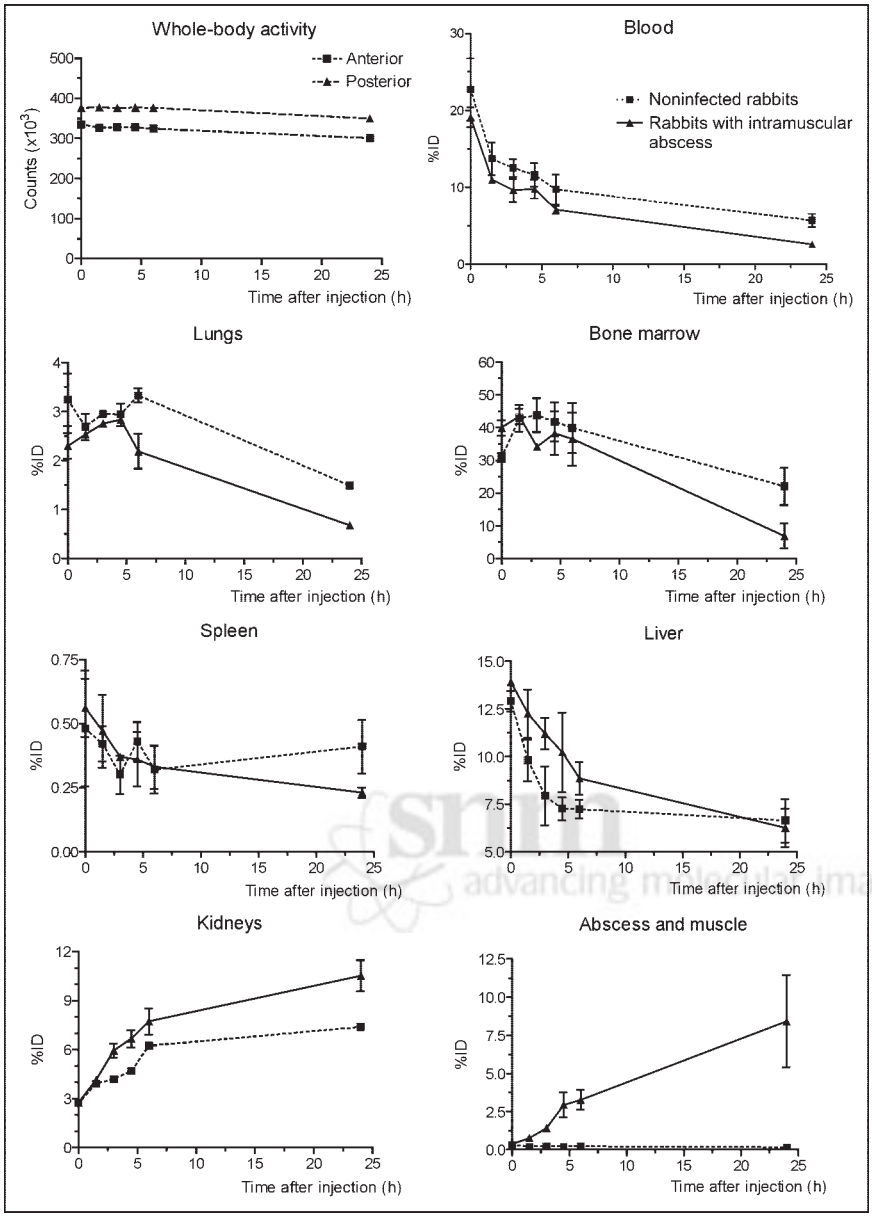

FIGURE 3. Dynamics of in vivo distribution of ^{111}In-DPC11870 in noninfected (healthy) rabbits and rabbits with intramuscular abscess. %ID was calculated on basis of whole-body activity and is represented for total body, total blood volume, lungs, bone marrow, spleen, liver, kidneys, total muscle, and abscess. Data are mean %ID ± SD.

marrow. With time, radioactivity cleared from these organs, except from the kidneys. Between 8 and 24 h after injection, the amount of ^{111}In-DPC11870 in spleen and liver remained stable, whereas activity concentrations continuously decreased in blood, lung, and bone marrow and increased in the *E. coli* abscess. Uptake of ^{111}In-DPC11870 in the abscess was low immediately after injection but increased continuously until 24 h after injection. When the pharmacodynamics of ^{111}In-DPC11870 in healthy rabbits were compared with those in animals with an intramuscular infection, differences in radioactivity concentrations were observed in blood, kidney, spleen, and bone marrow. Radioactivity concentration in the bone marrow was comparable in healthy and infected animals immediately after injection but radioactivity decreased more rapidly from the bone marrow of infected rabbits. Because blood levels were low from 4 h after injection and accumulation of radioactivity in the abscess occurred throughout the whole experiment (0–24 h after injection), the enhanced clearance of activity from bone marrow of infected animals suggested that ^{111}In-DPC11870 transferred from the bone marrow to the site of infection.

Studies to Determine Mechanism of Accumulation in Abscess

From the results of the pharmacodynamic studies and analysis of the %ID calculated from the ROI data, we hypothesized that accumulation of radioactivity at the site of infection might be due to migration of radioactivity originating from the bone marrow. To validate this hypothesis, healthy animals were injected with ^{111}In-DPC11870. At 16 h after injection, when the compound had cleared from the circulation almost completely (7.2 ± 0.9 %ID total

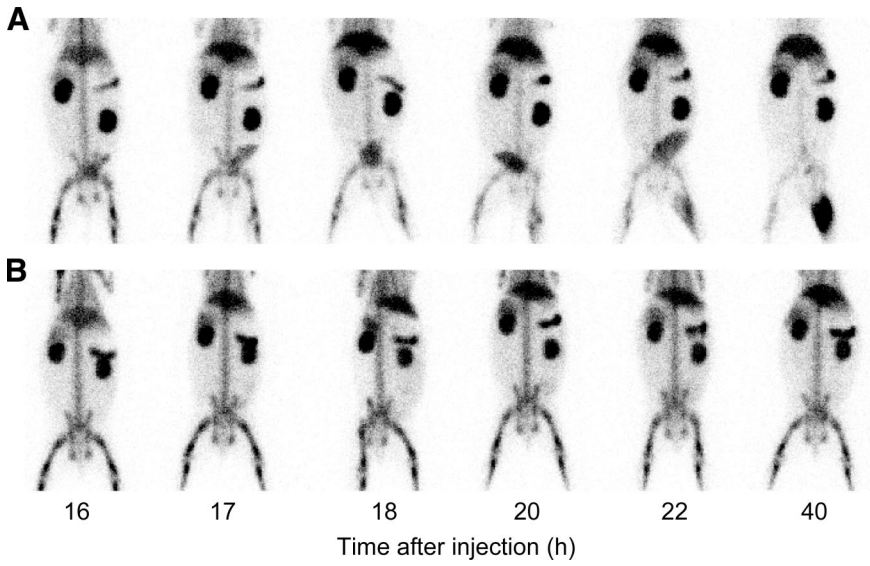

FIGURE 4. Anterior images of rabbits in which intramuscular infection was induced 16 h after injection of ^{111}In-DPC11870 (A) and healthy rabbits (B). Images were acquired from 16 h after injection of radiolabel (before induction of abscess) to 40 h after injection of radiolabel (24 h after induction of abscess).

blood-pool activity), animals were imaged and subsequently in 5 animals an intramuscular abscess was induced. At the time of dissection, at 40 h after the injection of ^{111}In-DPC11870, 2.9 ± 0.4 %ID and 2.2 ± 0.4 %ID of the radioactivity remained in the circulation of, respectively, healthy and infected animals ($P = 0.012$). Images acquired just before and at several time points after induction of the abscess are shown in Figure 4. The results of imaging before abscess induction (16 h after injection of ^{111}In-DPC11870) confirmed that the radioactivity concentration in the circulation (region over the heart) was low, whereas the concentration of the tracer in the bone marrow was relatively high. Subsequent images acquired after the inoculation of bacteria (Fig. 4A) showed substantial accumulation of radioactivity in the abscess. In these animals, some degree of visualization of the bladder was possible, indicating that a small amount of the injected dose was excreted via the urine. Comparison of these images with the images of animals that were not infected with *E. coli* (Fig. 4B) revealed that the radioactivity concentration in the bone marrow decreased more rapidly in infected animals and that ^{111}In-DPC11870 remained associated with the bone marrow in the healthy animals.

The results of the biodistribution were in concordance with the images (Table 1). At the time of tissue dissection (24 h after induction of the abscess, corresponding to 40 h after injection of ^{111}In-DPC11870), the amount of radioactivity in the bone marrow of healthy animals was 33.5 ± 4.3 %ID, whereas 9.2 ± 2.3 %ID was found in the bone marrow of the infected animals ($P < 0.0001$). The amount of radioactivity in the abscess was high (8.9 ± 2.5 %ID) and similar to the amount of radioactivity found in the abscess of infected animals injected with ^{111}In-DPC11870 24 h after induction of the abscess. The uptake of radiolabeled ^{111}In-DPC11870 in all other organs except the spleen was highly similar. The results of this experiment confirmed our hypothesis that accumulation of ^{111}In-DPC11870 in the abscess was due to migration of the tracer from the bone marrow. In addition, the results showed that radioactivity concentration in the bone marrow of healthy rabbits was more retained since the radioactivity concentration in the bone marrow of healthy animals was higher than in animals with an intramuscular abscess.

^{111}In-DPC11870 Bound to WBCs and BMCs

The mechanism of accumulation of radioactivity in the infectious foci was further investigated in a third experiment. In this experiment, we determined whether ^{111}In-DPC11870 bound to WBCs or BMCs was able to accumulate in the abscess. WBCs and BMCs were isolated from a donor rabbit with an intramuscular infection. After in vitro incubation of purified cells with 30 MBq of ^{111}In-DPC11870, initially 30% and 25% of the radioactivity was associated with WBCs and BMCs, respectively. After washing, more than 95% of the radioactivity was cell associated.

TABLE 1
Biodistribution of ^{111}In-DPC11870 in Rabbits 40 Hours After Injection

Site	Healthy animals	*E. coli*–infected animals*
Blood	0.02 ± 0.005	0.01 ± 0.003
Muscle	0.00 ± 0.001	0.00 ± 0.001
Femur	0.01 ± 0.006	0.01 ± 0.001
Marrow	0.75 ± 0.096	0.21 ± 0.050
Abscess		0.37 ± 0.161
Lung	0.08 ± 0.019	0.07 ± 0.021
Spleen	2.83 ± 0.413	1.35 ± 0.182
Kidneys	0.56 ± 0.120	0.66 ± 0.186
Liver	0.15 ± 0.033	0.15 ± 0.017
Intestine	0.01 ± 0.002	0.01 ± 0.002

*24 h after induction of abscess.
Data are %ID/g.

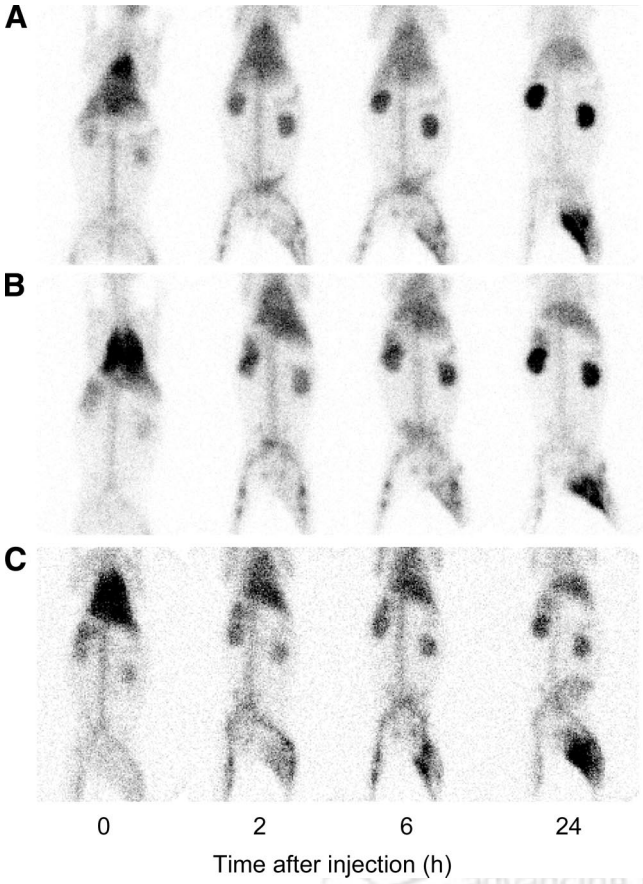

FIGURE 5. Anterior images of rabbits in which intramuscular infection was induced and 4 MBq of ^{111}In-DPC11870 (A), ^{111}In-DPC11870-BMCs (B), or ^{111}In-DPC11870-WBCs (C) were injected. Images were acquired immediately after injection of radiolabeled compound and at 2, 6, and 24 h after injection

Three animals with intramuscular *E. coli* infection were injected with either free ^{111}In-DPC11870, in vitro ^{111}In-DPC11870–labeled WBCs, or in vitro ^{111}In-DPC11870–labeled BMCs. Images were acquired at several times after injection. As shown in Figure 5, injection of ^{111}In-DPC11870 revealed images as obtained in previous experiments. The images obtained after injection of the in vitro–labeled WBCs and BMCs also demonstrated accumulation of radioactivity in the abscess. Visualization of the *E. coli* infection was similar for each of the 3 preparations. Furthermore, the early images showed transient entrapment of cell-associated radioactivity in the lungs. The images demonstrated that distribution of the different radiolabels was similar.

The biodistribution data showed that radioactivity concentrations in the various organs were similar except for the kidneys (Fig. 6). Kidney uptake of ^{111}In-DPC11870 and ^{111}In-DPC11870–labeled BMCs was 0.98 and 1.13 %ID/g, respectively, whereas uptake in the kidneys after injection of ^{111}In-DPC11870–labeled WBCs was much lower (0.54 %ID/g). Uptake of radioactivity in the kidneys represented loss or metabolized radioactivity. In all animals, radioactivity concentrations in the blood were low, and uptake in abscess was comparable (between 0.34 and 0.52 %ID/g).

DISCUSSION

In previous studies, we showed that the radiolabeled LTB4 antagonist DPC11870 efficiently revealed infection and inflammation in various rabbit models of infection and inflammation (*6,9,10*). In the present study, we determined the pharmacokinetics of ^{111}In-DPC11870 in detail and investigated the mechanism of accumulation in the abscess. Whole-body images confirmed previous findings concerning the rapid and distinct visualization of the abscess. The results of the pharmacodynamic analysis also showed that radioactivity in the bone marrow decreased more rapidly in infected animals than in healthy animals, in which radioactivity remained bound in the bone marrow. Besides the bone marrow, the lungs and the liver also showed decreasing radioactivity concentrations. However, the clearance rate in these organs was similar in healthy and infected animals and therefore could not cause the accumulation of radioactivity at the site of infection. Also, the differences in radioactivity

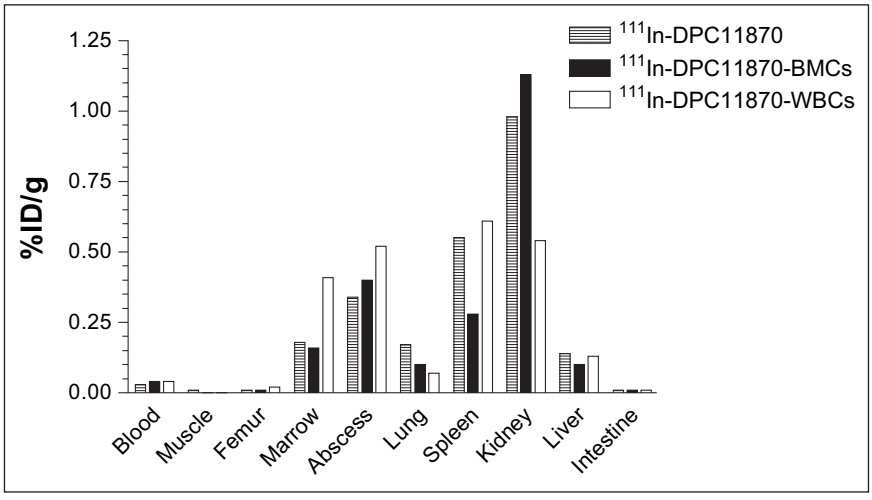

FIGURE 6. Biodistribution data obtained 24 h after injection of ^{111}In-DPC11870, ^{111}In-DPC11870-BMCs, or ^{111}In-DPC11870-WBCs. Data are %ID/g in individual organ or tissue.

concentration in the spleen between healthy and infected animals at 24 h after injection could not explain the uptake in the abscess, since the total amount of radioactivity in this organ is much different from the amount in the abscess. Because no other pharmacodynamic differences were found that correlated with the increasing abscess uptake, these results suggested that radioactivity from the bone marrow migrated to the abscess. We hypothesized that after injection, ^{111}In-DPC11870 targets receptor-positive cells and that because of subsequent migration of the tracer from the bone marrow, radioactivity accumulates in the abscess. To test this hypothesis, we injected ^{111}In-DPC11870 in healthy animals. Sixteen hours later an abscess was induced. Remarkably, at 24 h after injection of the radiolabel, radioactivity concentrations in the abscesses of these animals were similar to those of animals that were injected with the radiolabeled LTB4 antagonist after induction of the abscess (0.24 ± 0.08 %ID/g and 0.37 ± 0.16 %ID/g, respectively). In this experiment, a significant difference in clearance of radioactivity from bone marrow was found between animals infected with and animals not infected with *E. coli*. Images showed faster clearance of radioactivity from the bone marrow after induction of the abscess—a finding that is in line with the hypothesis of migration of a radiolabel from the bone marrow to the abscess. Apparently, induction of the abscess activated the immune system, with subsequent recruitment of BMCs to the site of infection. Biodistribution data further substantiated the hypothesis. The radioactivity concentration in the circulation of infected animals decreased by 4.5–5.0 %ID (similar to healthy animals), whereas almost 9 %ID of the radioactivity accumulated in the abscess during the same interval. Because the amount of radioactivity in the abscess was higher than the amount that had cleared from the circulation, and blood clearance was similar in healthy and infected animals, the radioactivity present in the abscess could not have originated from the circulation. Migration of (cell-associated) radioactivity from the bone marrow to the abscess could further explain the differences in radioactivity concentration in the bone marrow of infected animals and healthy animals at the time of dissection. At the time of dissection (40 h after injection of the radiolabel), the amount of ^{111}In-DPC11870 in the bone marrow of healthy animals was approximately 24% higher than that in infected animals (33.8 ± 4.5 %ID vs. 9.45 ± 2.5 %ID). As a result, this experiment demonstrated that our hypothesis was valid. The question remained, however, whether the radioactivity recruited from the bone marrow to the site of infection was cell associated. Therefore, in a third experiment we determined whether in vitro ^{111}In-DPC11870–targeted WBCs and BMCs could accumulate in the abscess. The images acquired after injection of the in vitro–labeled cells and unbound ^{111}In-DPC11870 were comparable and demonstrated that the in vitro–labeled cells also revealed the intramuscular abscess. Besides accumulation of radioactivity in the abscess, all 3 agents showed uptake in bone marrow and spleen and transient uptake in lungs. These findings agreed with the pharmacokinetics of radiolabeled WBCs (*13,14*). Studies that focused on the kinetics of radiolabeled WBCs showed that radiolabeled WBCs are temporarily trapped in the lungs and expose margination of activity in bone marrow and spleen. Additionally, accumulation of radioactivity in the kidneys of the rabbits was observed, indicating clearance of released ^{111}In-DPC11870. The biodistribution data confirmed that in vitro–labeled WBCs and BMCs accumulated in the abscess, comparable with ^{111}In-DPC11870. Furthermore, the biodistribution data revealed differences in radioactivity concentration in the spleen and kidneys. Uptake in the spleen indicated removal of cell-associated radioactivity and inversely correlated with radioactivity concentrations in the kidneys (released ^{111}In-DPC11870). Because the spleen is involved in removal of senescent granulocytes, uptake in this organ reflects splenic granulocyte destruction and explains the difference in uptake between healthy and infected animals (*15*). Because the turnover of granulocytes in healthy animals is much higher, this higher turnover leads to higher (cell-associated) splenic radioactivity concentrations in healthy animals than in infected animals, in which activated, in vivo–radiolabeled granulocytes are recruited to the abscess.

Although the in vitro–labeled BMCs and WBCs showed some release of radioactivity, because of similar imaging characteristics, comparable abscess uptake, high affinity of the LTB4 antagonist for its receptor (*6*), and expression of LTB4 receptors on immune cells (*16*), it is conceivable that accumulation of radioactivity in the abscess is mainly due to migration of cell-associated radioactivity. Moreover, in healthy animals the radiolabel remained associated with the BMCs that were present in this organ. Only at relatively early times after the injection of the radiolabeled compound, when blood levels are high, might there be a contribution from non–cell-associated activity that enters the site of infection and binds to receptors expressed by WBCs present in the abscess.

On the whole, our study indicates that visualization of infectious lesions with ^{111}In-DPC11870 is mainly due to accumulation of cell-associated radioactivity. The compound might therefore exhibit imaging characteristics similar to those of radiolabeled WBCs.

Because preparation of ^{111}In-DPC11870 is easy, rapid, and without potential risks, the disadvantages of preparing radiolabeled WBCs are absent. We therefore consider the radiolabeled LTB4 antagonist ^{111}In-DPC11870 a potential agent for visualizing infectious and inflammatory lesions in patients, and its investigation for applicability to clinical studies is warranted.

CONCLUSION

In this study, the pharmacodynamics of the radiolabeled LTB4 antagonist DPC11870 were investigated in detail. The results showed that radioactivity accumulates at the

site of infection mainly because of migration of ^{111}In-DPC11870 from the bone marrow and circulation to the abscess. It is convincible that migration of radioactivity to the site of infection is cell associated. Infectious foci can be visualized with ^{111}In-DPC11870 because of in vivo targeting of receptor-positive hematopoietic cells, and imaging characteristics resemble those of radiolabeled WBCs.

ACKNOWLEDGMENTS

The authors thank Gerry Grutters and Hennie Eijkholt (University of Nijmegen, Central Animal Laboratory) for technical assistance and Michel de Groot for assistance with the whole-body imaging experiments.

REFERENCES

1. Corstens FH, van der Meer JW. Nuclear medicine's role in infection and inflammation. *Lancet.* 1999;354:765–770.
2. Weiner RE, Thakur ML. Imaging infection/inflammations: pathophysiologic basis and radiopharmaceuticals. *Q J Nucl Med.* 1999;43:2–8.
3. Signore A, Chianelli M, Bei R, Oyen WJ, Modesti A. Targeting cytokine/chemokine receptors: a challenge for molecular nuclear medicine. *Eur J Nucl Med Mol Imaging.* 2003;30:149–156.
4. van Eerd JE, Boerman OC, Corstens FH, Oyen WJ. Radiolabeled chemotactic cytokines: new agents for scintigraphic imaging of infection and inflammation. *Q J Nucl Med.* 2003;47:246–255.
5. Rennen HJ, Corstens FH, Oyen WJ, Boerman OC. New concepts in infection/inflammation imaging. *Q J Nucl Med.* 2001;45:167–173.
6. van Eerd JE, Oyen WJ, Harris TD, et al. A bivalent leukotriene B(4) antagonist for scintigraphic imaging of infectious foci. *J Nucl Med.* 2003;44:1087–1091.
7. Toda A, Yokomizo T, Shimizu T. Leukotriene B4 receptors. *Prostaglandins Other Lipid Mediat.* 2002;68–69:575–585.
8. Yokomizo T, Izumi T, Chang K, Takuwa Y, Shimizu T. A G-protein-coupled receptor for leukotriene B4 that mediates chemotaxis. *Nature.* 1997;387:620–624.
9. van Eerd JE, Laverman P, Oyen WJ, et al. Imaging of experimental colitis with a radiolabeled leukotriene B4 antagonist. *J Nucl Med.* 2004;45:89–93.
10. van Eerd JE, Rennen HJ, Oyen WJ, et al. Scintigraphic detection of pulmonary aspergillosis in rabbits with a radiolabeled leukotriene B4 antagonist. *J Nucl Med.* 2004;45:1747–1753.
11. Gratz S, Rennen HJ, Boerman OC, et al. ^{99m}Tc-HMPAO-labeled autologous versus heterologous leukocytes for imaging infection. *J Nucl Med.* 2002;43:918–924.
12. Dams ET, Oyen WJ, Boerman OC, et al. Technetium-99m-labeled liposomes to image experimental colitis in rabbits: comparison with technetium-99m-HMPAO-granulocytes and technetium-99m-HYNIC-IgG. *J Nucl Med.* 1998;39:2172–2178.
13. Aktolun C, Ussov WY, Arka A, Glass D, Gunasekera RD, Peters AM. Technetium-99m and indium-111 double labelling of granulocytes for kinetic and clinical studies. *Eur J Nucl Med.* 1995;22:330–334.
14. Ussov WY, Aktolun C, Myers MJ, Jamar F, Peters AM. Granulocyte margination in bone marrow: comparison with margination in the spleen and liver. *Scand J Clin Lab Invest.* 1995;55:87–96.
15. Saverymuttu SH, Peters AM, Keshavarzian A, Reavy HJ, Lavender JP. The kinetics of ^{111}indium distribution following injection of ^{111}indium-labelled autologous granulocytes in man. *Br J Haematol.* 1985;61:675–685.
16. Pettersson A, Richter J, Owman C. Flow cytometric mapping of the leukotriene B4 receptor, BLT1, in human bone marrow and peripheral blood using specific monoclonal antibodies. *Int Immunopharmacol.* 2003;3:1467–1475.